Front. Environ. Sci. Eng. 2021, 15(6): 131
https://doi.org/10.1007/s11783-021-1419-1

RESEARCH ARTICLE

Influence of pore structure on biologically activated carbon performance and biofilm microbial characteristics

Yuqing Xu[1], Zedong Lu[1], Wenjun Sun (✉)[1,2], Xiaohui Zhang[3]

1 School of Environment, Tsinghua University, Beijing 100084, China
2 Research Institute for Environmental Innovation (Suzhou) Tsinghua, Suzhou 215163, China
3 Institute of Carbon Materials Science, Shanxi Datong University, Datong 037009, China

HIGHLIGHTS

- Pore structure affects biologically activated carbon performance.
- Pore structure determines organic matter (OM) removal mechanism.
- Microbial community structure is related to pore structure and OM removal.

ARTICLE INFO

Article history:
Received 1 October 2020
Revised 5 February 2021
Accepted 15 February 2021
Available online 5 April 2021

Keywords:
Granular activated carbon
Biologically activated carbon filter
Bacterial community structure
Pore structure

GRAPHIC ABSTRACT

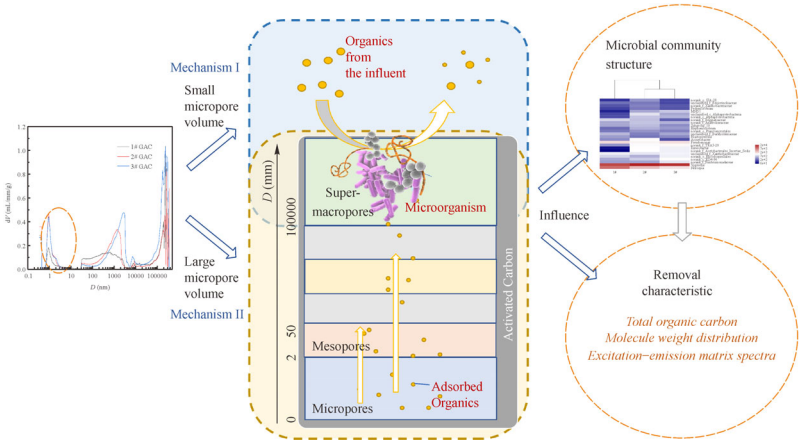

ABSTRACT

Optimizing the characteristics of granular activated carbon (GAC) can improve the performance of biologically activated carbon (BAC) filters, and iodine value has always been the principal index for GAC selection. However, in this study, among three types of GAC treating the same humic acid-contaminated water, one had an iodine value 35% lower than the other two, but the dissolved organic carbon removal efficiency of its BAC was less than 5% away from the others. Iodine value was found to influence the removal of different organic fractions instead of the total removal efficiency. Based on the removal and biological characteristics, two possible mechanisms of organic matter removal during steady-state were suggested. For GAC with poor micropore volume and iodine value, high molecular weight substances (3500–9000 Da) were removed mainly through degradation by microorganisms, and the biodegraded organics (soluble microbial by-products, < 3500 Da) were released because of the low adsorption capacity of activated carbon. For GAC with higher micropore volume and iodine value, organics with low molecular weight (< 3500 Da) were more easily removed, first being adsorbed by micropores and then biodegraded by the biofilm. The biomass was determined by the pore volume with pore diameters greater than 100 μm, but did not correspond to the removal efficiency. Nevertheless, the microbial community structure was coordinate with both the pore structure and the organic removal characteristics. The findings provide a theoretical basis for selecting GAC for the BAC process based on its pore structure.

1 Introduction

Biologically activated carbon (BAC) is widely used in the treatment of drinking water. When the available adsorption sites of activated carbon (AC) become saturated, the AC

✉ Corresponding author
E-mail: wsun@tsinghua.edu.cn

loses its adsorption capacity, and it is then said to be 'exhausted' (Korotta-Gamage and Sathasivan, 2017). Iodine value is a commonly used index to measure the adsorption capacity of activated carbon. Research has shown that the iodine value of GAC decreases with operation time (Liu et al., 2019). However, the organic contaminant removal efficiency of BAC remains stable within the first few years of use (Servais et al., 1994). The consistent removal capacity is attributed to the microorganisms.

According to Dussert and Stone (1994), the influent dissolved organic carbon (DOC) is removed by both adsorption and biological degradation, and the latter gradually becomes dominant. The biodegradation of natural organic matter (NOM) by BAC is a multi-step process; organic matter is first adsorbed by AC and is then partly degraded by the biofilm. The molecules that are not easily biodegraded diffuse into the pores of AC and are then modified into easily degradable ingredients by microbes, after which they undergo further microbial degradation (Dussert and Stone, 1994; Klimenko et al., 2002).

Factors affecting the treatment efficiency of BAC include water quality, temperature, AC characteristics, and operating conditions. These factors also impact the microbial characteristics of the biofilm.

Water quality, including nutrients and organic matter components, greatly influences the microbial community of BAC, especially for the poor nutrition environment of drinking water treatment. With different nutrient contents, the species diversity (Boon et al., 2011), microbial activity (Pharand et al., 2014), and dominant bacteria (Liao et al., 2013a) of the biofilm community also change. Under eutrophic conditions, the environment shows high selectivity for microorganisms, and hence has low population abundance (Liao et al., 2013b). BAC is reported to have better removal capacity for molecules with lower molecular weight; ozone is usually applied as a pretreatment to the BAC process to degrade molecules of high molecular weight into those with lower molecular weight (Xu et al., 2007). Temperature also influences BAC; at low temperatures (i.e., in winter), the removal capacity of BAC drops significantly, and the microbial characteristics such as community structure also change with temperature (Yang et al., 2014; Kaarela et al., 2015).

The microbial characteristics and removal capacity are largely related to the characteristics of the filter medium. In BAC filters, the AC type affects the biofilm community structure, and hence, the removal capacity. Chen et al. (2013) applied BAC columns with the only difference in GAC type, resulting in a difference in the dominant species and the microbial community structure in the effluent. Studies on the biomass and bioactivity of BAC have shown that increasing the macropore volume of GAC can protect the microorganisms attached to it from being destroyed by the shear stress of the water flow, thereby increasing the biomass (Pharand et al., 2014). The volume of the pores with diameter D greater than 100 μm determined the biomass and biological activity of the biofilm on GAC during stable operation (Yu, 2015). Study of Lu et al. (2020) suggested that the pore structure of GAC had a great impact on BAC performance through influencing the biofilm community structure, and that in a BAC filter, organics were removed by enzyme-driven adsorption. The important but previously unrecognized role of micro-level macropores (pores with diameters of 0.2–10 μm) was emphasized; they boost the bio regeneration ability of some GAC adsorption sites. Apart from the pore structure, surface polarity also influences the adsorption capacity of AC (Karanfil and Kilduff, 1999; Franz et al., 2000; Yapsaklı et al., 2009). However, no obvious relationship between surface polarity and BAC microbial characteristics has been reported, to the best of our knowledge.

The removal capacity and biofilm characteristics of BAC are also affected by the operation conditions of the BAC filter. It was found that the stability and richness of the biological communities in the up-flow filters were higher than those in the down-flow filters (Chen et al., 2013; Han et al., 2013). The service time of the column is also influential (Liao et al., 2013a); the longer the time, the more stable the biological community is (Chen et al., 2013). It was observed that it took 2–8 months for the biomass on a used BAC filter to adapt to new water quality (Ross et al., 2019). However, according to Du et al. (2020), younger carbons were associated with higher dissolved organic matter (DOM) removal efficiency.

Different researchers have different views on the removal characteristics and microbial characteristics at different heights of the carbon column. Some studies suggest that biomass density, bioactivity, and biodiversity decrease with increasing depth; however, others suggest that the indexes of microorganisms on BAC change little along the height (Pharand et al., 2014; Qi et al., 2018). Research (Chen et al., 2013) on up-flow AC filters showed that the distribution of HPC and ATP along the height was uniform, but the abundance of the dominant flora became higher in the effluent section. Hou et al.'s (2018) research on a full-scale drinking water treatment plant suggested that the results vary with season.

With the support of high-throughput sequencing technology, some progress in the determination of the biofilm community structure of BAC has been made in recent years. According to Lautenschlager et al. (2014), the common bacteria in the drinking water facilities studied were *Proteobacteria, Planctomycetes, Acidobacteria, Bacteriodetes, Nitrospira,* and *Chloroflexi.* These are all common bacteria found in natural water. In the pilot-scale study by Liao et al. (2013a) using 16S rRNA gene clone library analysis, *Alphaproteobacteria* was the largest

bacterial group present in BAC and is believed to be related to DOC and AOC removal. Hou et al. (2018) identified the dominant bacterial genera on BAC to be *Planctomycetes, Nitrospirae, Firmicutes, Bacteroidetes, Actinobacteria*, and *Acidobacteria.* Compared with other filters in the same drinking water treatment plant, the GAC filter enriched the *Bradyrhizobiaceae* and *Rhizobiales. Rhizobiales* aid the degradation of aromatics (Oh et al., 2018).

The properties of the BAC microbial community structure have been widely researched. However, the effect of GAC pore structure on the removal capacity and biofilm characteristics of BAC remains largely unknown. In this study, with the measurement of molecular weight distribution, excitation–emission matrix spectra and bacterial community structure, the characteristics, and mechanism of organic matter removed in BAC filters is analyzed. Aiming at discovering the impact of GAC pore structure on the removal capacity of BAC and microbial characteristics, this research provides new insights into the relationship between the pore structure of GAC, removal capacity of BAC, and microbial characteristics of the biofilm. The findings will guide the selection of GAC to be used in the BAC filter.

2 Materials and methods

2.1 Bench-scaled column experiments

2.1.1 Synthetic water preparation

The plant was fed with synthetic humic-rich surface water (average dissolved organic carbon (DOC) concentration — 2 mg/L).

Humic acid (FA⩾90%, CAS: 1415-93-6, Macklin, Shanghai, China) was first dissolved in a solution of 0.1 mmol/L NaOH to a 5 g/L stock solution, and was stored away from light at 4°C, in preparation for use.

When needed, the stock solution was diluted with tap water (Wu et al., 2012) so that the applied solution had a DOC of approximately 2 mg/L; 0.1 mol/L HCl was added to maintain the pH of the influent in the 6.8–7.2 range.

2.1.2 GAC selection

Each type of GAC was measured for the static adsorption capacities of humic acid. 0.16, 0.32, 0.64 and 1.28 g of GAC were mixed with humic acid solution (DOC = 1.6 mg C/L). After oscillation for 24 h at 25°C, the DOC of each solution was tested. Three types of GAC with the best DOC removal efficiency were selected.

The selected GAC types were: Shaanxi carbon, Huaqing carbon, and Calgon carbon, hereafter called 1#, 2#, and 3# GAC, respectively. All of them are coal-based AC. Huaqing carbon and Calgon carbon are widely used in drinking water treatment because of their high iodine values.

2.1.3 Experimental setup

The bench-scale plant included three glass GAC columns, 0.03 m × 0.65 m, which were connected in parallel to the raw water tank. The columns were sequentially filled with three types of carbon of the same particle size (8 × 30 mesh) to 30 cm depth, all of virgin carbon.

The height of the filled GAC column was 30 cm, and a 5 cm quartz gravel supporting layer was added in the lower part of the carbon column. The operation mode of the carbon column was downward flow. An overflow pipe was provided 15 cm above the GAC layer which also acted as an outlet during backwash.

A peristaltic pump was used to control the flow rate of the influent, keeping the empty bed residence time of the carbon columns at 25 min. The outlet pipe of the carbon column is folded upwards so that the highest point is 15 cm above the surface of the GAC layer. The scheme of the GAC column is shown in Fig. 1.

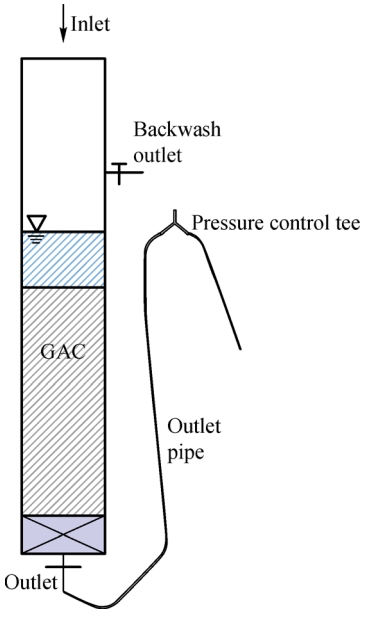

Fig. 1 Scheme of a BAC column.

In the early stage of the experiment, the water inlet was continuously adjusted to maintain a stable water inlet rate, and the water outlet was adjusted for convenient sampling.

Since the influent DOC, hydraulic load (Servais et al., 1994), empty bed contact time (McKie et al., 2019), and particle size of GAC (Du et al., 2020) are known to affect the biomass density, biological activity, and diversity of the biological community, this study maintains influent water quality, water inflow rates, and the GAC particle size in the three carbon columns consistent.

2.2 Sampling and analysis

2.2.1 GAC pore structure measurement

According to the Dubinin division method, the pores of GAC can be divided into the following categories: $D>$ 50 nm, macropores; D = 2–50 nm, mesopores; $D<2$ nm, micropores.

The GAC in the three columns was first completely dried at 120°C. The volume of macropores (pores with a diameter of more than 50 nm) was measured by mercury intrusion with an AutoPore IV9500 (Micromeritics, USA) (Morlay and Joly, 2010). Although the results of Hg intrusion range from 3–370000 nm, the volume of mesopores and micropores (pores with a diameter of less than 50 nm) was measured by gas adsorption for higher accuracy, using an Autosorb-i Q2-MP (Quantachrome, USA) at 77 K, which gives out the pore volume with a corresponding pore diameter of 0.2–190 nm. The mesopore volume distribution was determined based on the BJH model and the micropores on the H-K-S-F model (Lu et al., 2020), detailed in Appendix A (Supporting Information).

Based on the pore volume distribution measured by the above methods, macropores were further divided into micro-level macropores (D = 200–10000 nm) and super-macropores ($D>100$ μm). The distribution criterion was more detailed discussed in Section 3.1, based on Fig. 2.

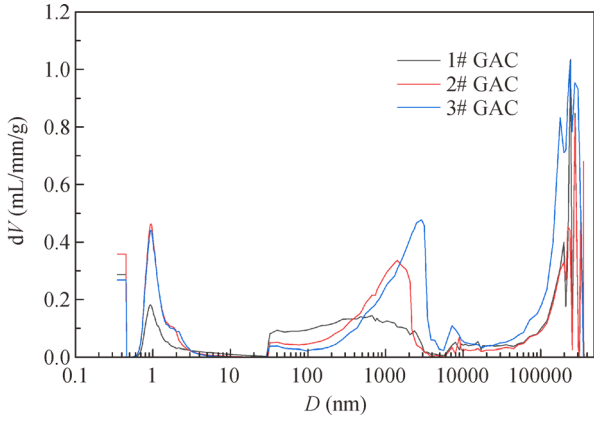

Fig. 2 Pore volume distribution of the three types of GAC.

2.2.2 Dissolved organic carbon (DOC) assay

A total organic carbon analyzer (Aurora 1030, OI Analytical, College Station, TX, USA) was used to determine the DOC of the influent and effluent. Before testing, all samples were filtered through a 0.45 μm membrane. Water samples were analyzed in triplicate to ensure accuracy.

2.2.3 Molecular weight (MW) distribution assay

A high-performance size-exclusion chromatography (HPSEC, Waters, USA) was used to measure the MW distributions of the organic matter in the influent and the effluent, as described in our previous study (Lu et al., 2020). All the samples were filtered through a 0.45 μm membrane before testing. Water samples used for MW distribution assay were collected on day 100 of the experiment.

2.2.4 Excitation–emission matrix (EEM) spectra assay

A HITACHI F-7000 fluorescence spectrophotometer (Tokyo, Japan) was applied to conduct the EEM scanning. The excitation wavelength was set at 200–500 nm, while the emission wavelength was set at 250–600 nm, both at 2 nm intervals, with a scanning speed of 2400 nm/min. The contour maps of the EEM were plotted via Origin 2018 (OriginLab, USA). When calculating the fluorescence regional integration, deionized water was used as the blank (Jiang et al., 2013; Zheng et al., 2018). Before testing, all samples were filtered through a 0.45 μm membrane. Water samples used for EEM scanning were collected on day 105 of the experiment.

2.2.5 Quantification of the bacterial biomass

The biomass density of surface GAC was measured every two to three weeks by the heterotrophic plate count (HPC) method, and 0.5 g of the surface layer of the GAC filtration bed was adopted for the extraction of the biomass. After applying to 15 mL of sterile water, the GAC samples were sonicated for 10 min. Then, the supernatant was diluted by gradient and cultured on R2A plates at 22°C for 7 days (Han et al., 2013; Lu et al., 2020). The biomass density was determined according to the number of colonies on the plates and the corresponding dilution ratio. Samples were analyzed in triplicate to ensure accuracy.

2.2.6 Microbial community structure assay

Fifteen biomass samples (each weighing 3 g) were collected from three different heights of each BAC filter column on day 110. The pretreatment of the samples, the extraction of DNA (via the Axygen bacterial genomic DNA extraction kit), and the polymerase chain reaction (PCR) amplification of 16S rDNA were performed in consistent with Lu et al. (2019). The primer pair of PCR was 515F (GTGCCAGCMGCCGCGG) and 907R (CCGTCAATTCMTTTRAGTTT). The high-throughput sequencing was conducted via an Illumina Hiseq platform (Majorbio Bio-Pharm Technology Co., Shanghai, China). The accession numbers of sequence data deposited in the NCBI SRA database were SRR11805431- SRR11805440.

Quality control of the original sequencing sequence was conducted via Fastp (version 0.19.6, Haplox Biotechnology, China), and merging of the raw data was conducted

via FLASH (version 1.2.11, Center for Computational Biology, Johns Hopkins University, USA) (Magoč and Salzberg, 2011; Chen et al., 2018). The criteria were as follows: 1) Reads whose quality score was less than 20 were discarded, and a 50 bp sliding window was set. If the truncated read was shorter than 50 bp, or contained ambiguous characters, they were discarded as well; 2) According to the overlapping relationship between paired-end reads, the paired reads were merged into a sequence, and the minimum overlap length was 10 bp; 3) The maximum mismatch ratio of overlap region was 0.2, and the unmatched sequences were discarded; 4) The sequence direction was adjusted. The allowed number of mismatches in the barcode was 0, and the maximum number of primer mismatches was 2.

UPARSE 7.0.1090 (RC Edgar, USA) was applied to cluster the operational taxonomic units (OTUs) with a 97% similarity cutoff, and chimeric sequences were identified and removed (Stackebrandt and Goebel, 1994; Edgar, 2013). The taxonomy of each OTU representative sequence was analyzed using RDP Classifier 2.11 (Center for Microbial Ecology, Michigan State University, USA) with the 16S rRNA database SILVA v132 (Microbial Genomics and Bioinformatics Research Group, and Ribocon GmbH, Germany), and the confidence threshold was 0.7 (Wang et al., 2007).

3 Results and discussion

3.1 GAC pore structure and surface polarity properties

The pore diameter distribution is shown in Fig. 2. The micropores ($D < 2$ nm, D for diameter), mesopores ($D = 2$–50 nm), and macropores ($D>50$ nm) were divided by the Dubinin method. Besides, based on the peaks in Fig. 2, the macropores were further divided into micro-level macropores (D = 200–10000 nm, the second peak) and super-macropores ($D>100$ μm, the third peak). The reason why the lower limit of the diameter range of micro-level macropores was 200 instead of 50 was: the smallest bacterial cell size is approximately 200 nm, so pores with D greater than 200 nm deserve more attention (Lu et al., 2020). The porosity and iodine values of the three GAC samples are shown in Table S1.

For micropore volume, 2# Huaqing and 3# Calgon were similar, greater than for 1# Shaanxi; 1# had an approximately 35% lower iodine value and a 50% lower micropore volume than 2# and 3#; mesopore volume of 2# and 3# were also similar, smaller than for 1#; for micro-level macropores (D = 200–10000 nm), 3#>2#>1#, and for super-macro pores ($D>100$ μm), the pore volume of 3#>1#>2#.

The first peak of pore volume in Fig. 2 was composed of micropores and mesopores. The micropore and mesopore volume distributions of 2# and 3# GAC were similar, while the pore volume of 1# was significantly lower than that of the other two. The micropore volume peaks of the three types of GAC were all near the pores with a D of 1 nm. Within the mesopores, all three types of carbon had larger pore volumes at small pore sizes. The distributions of 2# Huaqing and 3# Calgon carbon were similar, and the pore volume consisted largely of pores with $D < 10$ nm; 1# Shaanxi carbon was relatively uniform, with pore volume distribution concentrated along the 2–30 nm diameter range.

The distribution of micro-level macropores in 1# Shaanxi GAC was relatively low and uniform, while 2# Huaqing and 3# Calgon had relatively high and concentrated pore volumes. The pores of 3# Calgon were the most developed in the range of micro-level macropores and super-macropores.

The adsorption capacity of AC is also related to its surface chemical properties (Yapsaklı et al., 2009). Studies have shown that phenolic hydroxyl groups and carboxylic acid groups are the main groups determining the surface acidity of AC. These chemical groups can reduce the adsorption capacity of organic compounds in water (Karanfil and Kilduff, 1999; Franz et al., 2000). Research by Lu et al. (2020) suggests that the summation of hydroxyl and carboxyl groups is similar for the three types of GAC (Table S2). Due to the lack of difference in the surface polarity among the three types of GAC, the difference in the removal characteristics and microbial characteristics are mainly attributed to the difference in the pore structure of the GACs.

3.2 Organic matter removal characteristics

DOC was used to characterize water quality, and the DOC removal efficiency was used to assess the effectiveness of organic matter removal. At the beginning of the process, the ranking for organic matter removal efficiency was 3#>2#>1#. Subsequently, the removal efficiency of the 2# and 3# BAC columns decreased significantly, while the organic matter removal efficiency of the 1# BAC column increased and then decreased (Fig. 3).

During the entire operation, the removal efficiency curves for 2# BAC and 3# BAC were relatively close compared to that of 1#, similar to the difference of pore structure between the GACs. After the removal efficiency stabilized, the removal efficiency of 1# carbon was about 32%, and those of 2# and 3# were at about 27%, with the removal efficiency of 3# slightly higher than that of 2#. The difference in DOC among the effluents of the three was within 0.1 mg/L.

A backwash was performed on the 70th day of the study. As is shown in Fig. 3, after backwashing, the organic matter removal efficiency first decreased before recovering and exceeding the former rate. The brief reduction in removal efficiency after backwashing was due to the decrease in biomass (Liu et al., 2016), and the subsequent

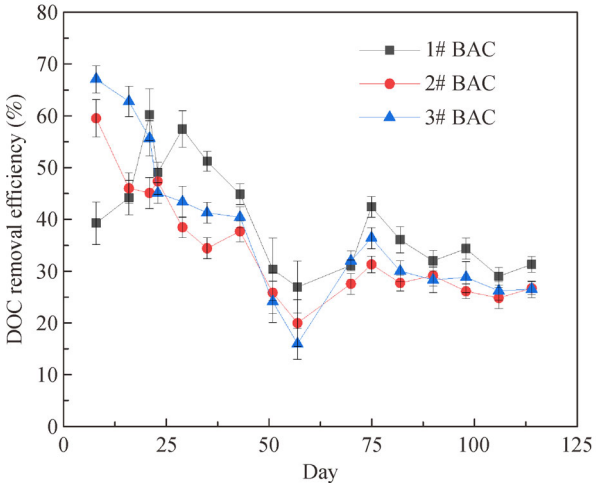

Fig. 3 Dissolved organic carbon removal with time.

increase in removal efficiency was attributed to the increased biological activity (Chen et al., 2013; Liao et al., 2013b).

Although GAC with very different iodine values and developed pores had similar total organic removal efficiency after the establishment of stable operating conditions, they had different removal capacities for different organic fractions. The influent DOC was mainly distributed in the range of 2000–8000 Da, with a peak at approximately 4500 Da (Fig. S1). The percentage removal efficiency of organics within different MW intervals are listed in Table 1.

The percentage reduction of each organic fraction was calculated according to Hidayah et al. (2016). The rank of total reduction percentage (Table 1) was the same as the rank of DOC reduction (Fig. 3).

As shown in Table 1, 2# BAC and 3# BAC had better removal efficiencies for molecules with MW < 3500 Da; however, their removal efficiency for molecules in the range of 3500–8900 Da was much lower than that of 1# BAC. In contrast, 1# BAC had a high removal efficiency for 3500–8900 Da molecules but could not effectively remove the molecules with MW less than 3500 Da.

EEM regions are shown in Table S3 according to Chen et al. (2003), and the results of three-dimensional fluorescence spectroscopy are shown in Fig. S2. The fluorescence intensity was normalized by the fluorescence intensity of the humic acid-like substances in the influent. The change in fluorescence intensity is demonstrated in Fig. S3, and the percentage reduction in fluorescence intensity is listed in Table 2. The three types of BAC mainly remove humic acid-like and fulvic acid-like substances, and for humic acid-like substances, 2# and 3# BAC had better removal efficiency than 1#. Moreover, 1# BAC could not remove microbial by-products and aromatic proteins I and II effectively; in contrast, the concentration of these organics increased. BAC 2# and 3# had a fluorescence intensity reduction of 11.0% and 15.6% for microbial by-products, respectively. The fluorescence intensity reduction of 2# and 3# BAC for aromatic proteins I and II were both close to 0. The removal pattern of microbial by-products was similar to the removal characteristics for molecules with MW less than 3500 Da. On the other hand, soluble microbial by-products are bacteria-produced DOM (Chen et al., 2003). The high removal efficiency of total DOC by 1# BAC may be attributed to high biological activity (which is in turn attributed to the community structure). However, due to the poor adsorption by micropores, the by-products produced by microbes could not be removed. Inferred from above, the molecules that cannot be removed by 1# but can be partly removed by 2# and 3# BAC may be classified as soluble microbial by-products.

However, while 1# Shaanxi BAC had the highest DOC removal efficiency among the three (which corresponded to the total removal efficiency calculated by MW distribution in Table 1), the effluent of 1# BAC had the highest fluorescence intensity. This may be attributed to the different perspectives between EEM and DOC. EEM

Table 1 Organic fraction removal by BAC filtration using HPSEC-UV

Organic fractions (%)	< 3500 Da [a)]	3500–8900 Da [a)]	Total [b)]
Percentage reduction of 1# BAC	–0.49	40.34	39.85
Percentage reduction of 2# BAC	12.87	8.98	21.86
Percentage reduction of 3# BAC	13.95	12.85	26.80

Notes: The MW of the organics was divided by 3500 Da because, as seen in Fig. S1, the removal characteristics of organics change with 3500 Da as a boundary. a) Percentage reduction in each fraction = [(Area of specific fraction range)$_{influent}$ – (Area of specific fraction range)$_{effluent}$]/ [(Total area)$_{influent}$ – (Total area)$_{effluent}$] × % removal of total area. b) Percentage reduction in total area between influent and BAC treated water.

Table 2 Fluorescence intensity reduction of each region after BAC treatment (%)

No.	Humic acid-like	Fulvic acid-like	Microbial by-product	Aromatic Protein I and II
1#	49.1	32.2	–45.0	–17.7
2#	65.2	39.8	11.0	–0.2
3#	66.7	35.8	15.7	0.4

provides a perspective of the functional groups; EEM fluorescence intensity has some correlation with DOC and MW but is not completely consistent. Some functional groups that have not been removed by BAC may contribute less to the DOC content.

It should be noted that, although the total removal efficiency of the three types of BAC was similar, the removal efficiency of different kinds of substances and different molecular weights were different, so appropriate activated carbon should be selected according to the quality of the water to be treated.

The differences in removal characteristics of 1# vs 2# and 3# BAC, reveals a difference in the removal mechanism, as discussed in Section 3.4.

3.3 Factors affecting removal efficiency

The GAC columns were operational for approximately 3 months before the DOC removal efficiency and biomass density stabilized. After stabilization, organic matter was removed by both adsorption by GAC and decomposition by microorganisms (Korotta-Gamage and Sathasivan, 2017).

3.3.1 Adsorption capacity

As is shown in Fig. S4, the static adsorption capacities of the three types of GAC were similar and were not in line with the adsorption capacities at the beginning of the operation, or the removal capacities in the steady stage.

Research on the full-scale GAC based drinking water plant showed that the process of removal of small-molecule organic matter in NOM is more efficient than that of large-molecule organic matter, because small-molecule organic matter enters and diffuses through the pores of GAC more easily (Gibert et al., 2013). Micropores of GAC play the main role in the removal of small organic molecules (Chiang et al., 2001; Lillo-Ródenas et al., 2005). The micropore volume of 1# GAC was significantly smaller than that of 2# and 3# GAC. Therefore, the poor removal capacity of 1# carbon with respect to small MW (<3500 Da) organic molecules may be due to its small micropore volume, which results in low adsorption capacity.

While micropores contribute most to the adsorption of molecules with low MW, mesopores are found to contribute to the removal of molecules with higher MW (Newcombe et al., 1997; Moore et al., 2001). The MW of the influent was mainly in the 2000–9000 Da range. According to Moore et al. (2001) and Newcombe et al. (1997), in this range of MW, the mesopores of AC play an important role in the removal of organic molecules. Although the total micropore volume of 1# GAC was lower than those of 2# and 3#, it had a much higher mesopore volume (Table S1), which might be responsible for the higher DOC removal efficiency.

3.3.2 Microbial characteristics

3.3.2.1 Biomass density

After the carbon column operated for approximately 3 months, both the organic matter removal efficiency and the biomass became stable. The surface carbon was extracted to measure the stabilized biomass, on day 110 of the columns becoming operational.

Examination of the stabilized biomass density for the pore volume of super-macropores ($D>100$ μm) revealed that GAC with a greater super-macropore volume had larger biomass attached to it (Fig. 4). This result was consistent with Yu's (2015) finding; however, in this study, the correspondence did not show linearity.

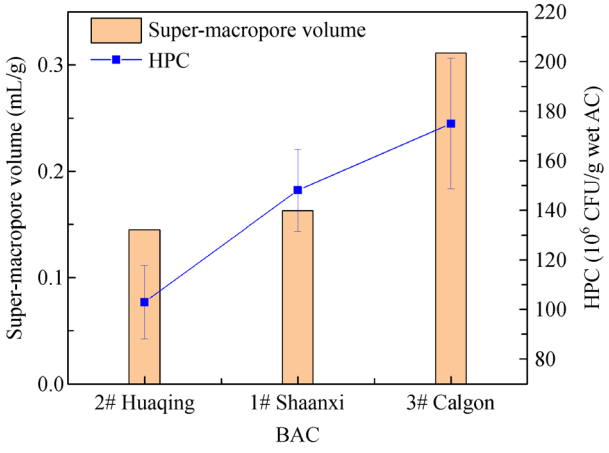

Fig. 4 HPC corresponding to the super-macropore volume.

Comparison between biomass density with removal capacity (Fig. 3) showed that a higher biomass density did not guarantee a higher DOC removal efficiency. This is consistent with the conclusion of Lu et al. (2020). A similar situation has been addressed in the study by Herzberg et al. (2006). The study compared the removal efficiency of NOM and the biomass of AC with inactivated carbon and found that the removal efficiency of the two were similar, but that the biomass of AC was significantly higher than that of inactivated carbon. The authors speculate that this is due to the higher loss of biomass in the inactivated carbon, which is attributed to the higher wash-out rate. This can also explain the relationship between biomass and removal efficiency in this study; that is, more biomass on GAC with a smaller super-macropore volume was washed out than biomass on GAC with a larger super-macropore volume, resulting in a large difference in biomass when the DOC removal efficiency was similar.

3.3.2.2 Microbial community structure

The total number of bacteria genera on 1#, 2#, and 3# BAC was 367, 372, and 396, respectively (Fig. S5), which was

consistent with the rule that the larger the super-macropore volume is, the more bacterial genera get attached to the GAC. The number of the distinct genera on 3# BAC was the largest, namely 36 genera, which were higher than for 1# (15 genera) and 2# (13 genera). The number of genera was not consistent with the removal efficiency of organic matter by BAC.

Therefore, while the super-macropore volume was consistent with the biomass density and the number of genera, and neither biomass density nor the number of genera was consistent with the removal capacity, the super-macropore volume did not prove important for organic matter removal.

According to the OTU curves, the rank of biodiversity was 2#>1#>3# (Fig. S6). There was no correlation between biodiversity and the performance of BAC. The result agrees with Yang et al. (2016).

The communities of 2# and 3# BAC at the water outlet sections were closer, observed from both phylum level (Fig. S7) and genus level (Figs. 5(a) and 5(b)). The dominant phylum or genus of the three carbon columns were the same. In the outlet section, the dominant genus was *Vogesella*, accounting for 37.6%, 46.8%, and 45.1% for 1#, 2#, and 3# BAC, respectively. *Nitrospira* was the next, accounting for 22.9%, 5.83%, and 4.13%, of which 1# BAC was significantly different from 2# and 3#. At the phylum level, the dominant phylum was *Proteobacteria*, which accounted for 62.6%, 78.2%, and 78.4% for 1#, 2#, and 3# BAC, respectively, followed by *Nitrospirae*, which accounted for 22.9%, 5.8%, and 4.1%, respectively.

It should be noted that the removal characteristics (including the removal efficiency, effluent MW distribution, and EEM fluorescence intensity) of 2# and 3# BAC were similar, and the pore structures of these two GAC

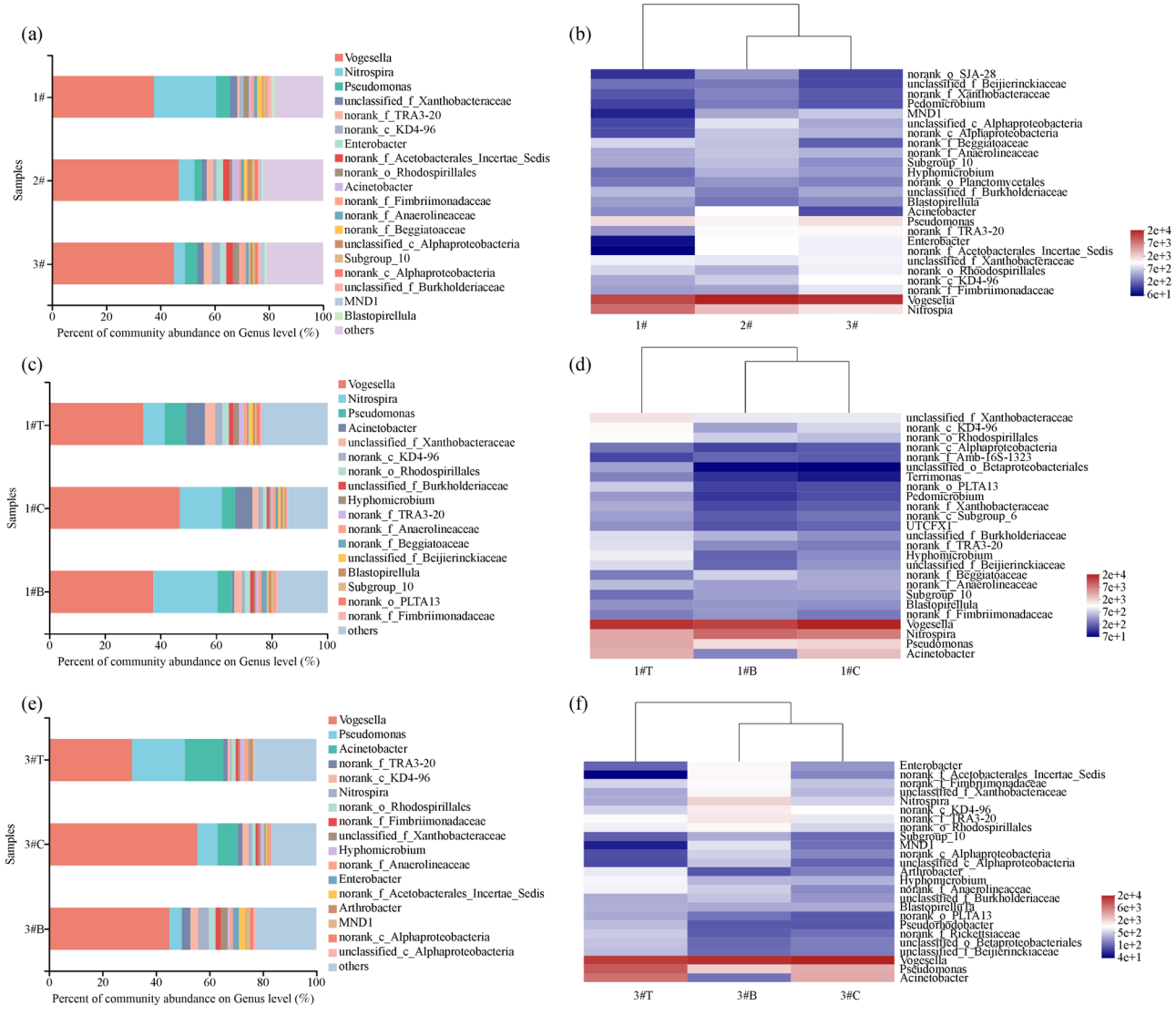

Fig. 5 Community structure of the BAC biofilm samples: T is top, C is central and B is bottom; (a) Barplot of three outlet sections, (b) Community heatmap of three outlet sections, (c) and (d) Barplot and heatmap of 1# BAC samples from different heights on the column, (e) and (f) Barplot and heatmap of 3# BAC samples from different heights on the column.

columns, apart from the super-macropores' (D>100 μm) volume, were also relatively close.

Because of the similarity in the removal characteristics and the community structure, the community structure was speculated to affect the removal capacity. The high removal efficiency of 1# BAC may be attributed to its biofilm community structure, which was supposed to be more adapted to the degradation of molecules with higher MW.

Miro-level macropores and super-macropores were the only pore type with a concentrated pore volume that microorganisms could enter. Due to the lack of consistency between community structure and super-macropores, and integrated with the conclusion of Lu et al. (2020), it could be speculated that the community structure was primarily affected by the volume and distribution along the diameter of micro-level macropores.

The community structure of the 3# BAC indicated that a higher proportion of the dominant genus did not guarantee a higher organic matter removal efficiency. The reason might be that the bacterial species with the highest proportion need not necessarily have the highest organic matter metabolism (Oh et al., 2018).

3.4 Organic matter removal mechanisms

Based on the factors mentioned in Section 3.3, the process of organic matter removal is summarized as follows:

At the beginning of the operation, before the micro-organisms start degrading the organic matter effectively, the organics were mainly removed by adsorption by the AC. Subsequently, in accordance with the MW and EEM results, the stable state removal mechanism of 1# Shaanxi BAC differed from that of 2# Huaqing and 3# Calgon, while the mechanism of 2# and 3# BAC were similar. Based on the pore structure and microbial community structure difference, the removal mechanism of 1# BAC in the stable period can be described as follows: 1# BAC mainly decomposed large-molecule organic matter into small-molecule organic matter; the adsorption of 1# GAC was underdeveloped, so the degraded small-molecule organic matter was not efficiently removed. According to the MW distribution and EEM results, these fractions were most likely soluble microbial by-products, with MW less than 3500 Da. The microbial community structure of 1# BAC had a relatively big difference compared to that of 2# and 3# BAC. Hence it could be speculated that it was the microbial community structure of 1# BAC that enhanced the organic removal of larger molecular organics (MW>3500 Da). As a result, 1# BAC was more adapted to the removal of larger molecular organics. The removal mechanism of the other two types of BAC was similar: the organics adsorbed in the pores of GAC were degraded by microorganisms; this released the adsorption sites which can then adsorb more organics. As physical adsorption mainly removed small molecular organics, the removal efficiency of molecules less than 3500 Da was high.

According to the biological regeneration theory for BAC, microorganisms use organic substances adsorbed by AC and accumulated in the pores (Korotta-Gamage and Sathasivan, 2017). This model was improved by Lu et al. (2020) as follows:

First, the organics are adsorbed into the pores of GAC. Microorganisms secrete enzymes that enter the macropores or mesopores, and degrade the organics present in these pores. Then, because of the concentration gradient of organics between micropores and pores with a larger diameter, organics adsorbed in micropores can diffuse into mesopores and macropores, where they are degraded. In this process, the adsorption capacity of micropores is renewed, so that BAC can remove organics for a long period of time without being exhausted. Micro-level macropores play an essential role in the diffusion of enzymes, and thereby boost the bio regeneration ability of GAC adsorption sites.

This theory could be applied to explain the removal characteristics in this study. Regarding the difference in pore structure and organic removal characteristics, this study could, in turn, provide some improvement to the theory.

Relating the above-mentioned removal mechanisms to the pore structure, two possible mechanisms by which the organics are removed in BAC could be summarized as follows:

Mechanism I: Microorganisms themselves degraded organic matter; large molecules were degraded into small molecules or carbonized, and the degraded molecules were possibly soluble microbial by-products with MW less than 3500 Da. This mechanism mainly contributed to the removal of larger molecular weight organics. The community structure of the microorganisms greatly influenced the removal capacity.

Mechanism II: Diffusing through the micro-level macropores, enzymes removed the organic matter adsorbed in the micropores and diffused to mesopores and macropores. This created a concentration gradient that promoted the diffusion of organics. In this process, the adsorption sites of GAC were continuously released, so that adsorption continued to contribute to organic matter removal during the stable stage. This mechanism mainly contributed to the removal of organics with smaller MW.

These mechanisms are illustrated in Fig. 6. The organic removal by 1#, 2#, and 3# BAC could be explained by the mechanisms as follows:

The larger micropore volume of 2# and 3# BAC led to higher adsorption capacity, while 1# BAC could only adsorb a small amount of organics due to its insufficient micropore volume. As a result, the biofilm of 2# and 3# BAC could obtain adequate organic from mechanism II,

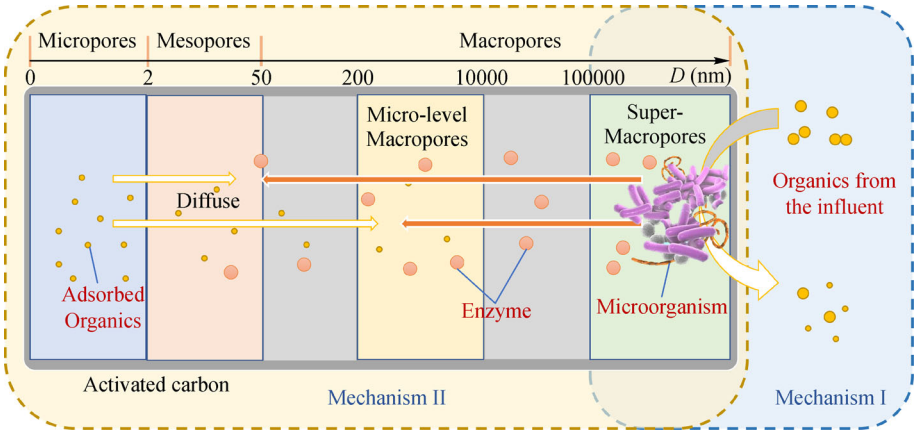

Fig. 6 Schematic diagram of the two organic removal mechanisms.

while the biofilm of 1# BAC could not. Thus, the biofilm of 1# BAC tended to obtain organic matter from the solution through mechanism I.

The most important pores of GAC were hence micropores and micro-level macropores. The micropores affected the adsorption, and the micro-level macropores affected the diffusion and community structure of the biofilm; both the total volume and the volume distribution of micro-level macropores (Fig. 2) may be influential.

3.5 Community structure analysis

The microbial community structure could be determined by the GAC pore structure, and the removal capacity of BAC was in turn influenced by the community structure (Section 3.3). As a result, the three types of BAC had different removal characteristics for different organic fractions. The difference in community structures of the BAC types may be because the biological community structure of 1# BAC was more conducive to the degradation of macromolecular organic matter than the community of 2# and 3#, but due to the poor iodine value of GAC itself, the smaller MW organic matter after degradation was not adsorbed, but released into water. Community structure is thus analyzed in this section regarding the community structure and its distribution.

3.5.1 Biodiversity

In general, the relative biodiversity in the 3 BAC types, from high to low, was: 2#>1#>3# (Fig. S6), which was the opposite of biomass ranking. There was no correlation between the biodiversity of the sample and its location in the column.

The difference in biodiversity between carbon samples at different positions of the same carbon column was small, while the difference among carbon columns was relatively large. The results agree with the conclusion of Chen et al. (2013).

3.5.2 Dominant genus

Vogesella was the dominant bacterial genus in all samples from different heights of the three carbon columns. In some samples, *Vogesella* accounted for more than 50% of the microbial community. Identification of the two *Vogesella* strains revealed their evolutionary tree, as shown in Fig. 7. *Vogesella* formed indigo blue colonies on R2A plates, some of which had a white center.

The dominant genera of the three BAC samples were similar, but their proportions were different. *Acinetobacter* accounted for a small proportion in 2#, but a higher proportion in 1# and 3#. Among 1# and 2# BAC,

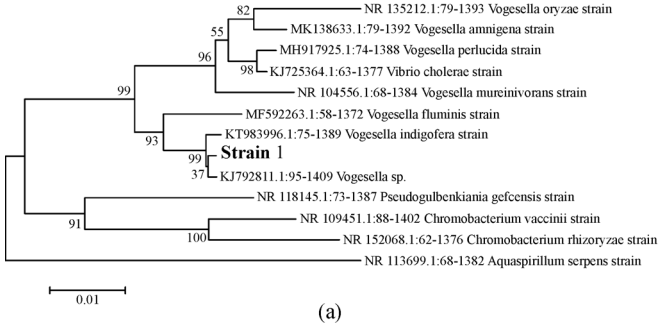

Fig. 7 Evolutionary tree of two *Vogesella* strains: (a) Strain 1; (b) Strain 2.

Nitrospira accounted for a significantly higher proportion than in 3#, while *Pseudomonas* accounted for a higher proportion in 3#. As 1# and 2# GAC had a closer super-macropore volume, it could be speculated that the proportion of the dominant genus was related to the properties of AC, possibly the super-macropore volume.

The above results for dominant bacteria were inconsistent with the research findings on the bacterial community in drinking water plants by Chen et al. (2013) and Lautenschlager et al. (2014). *Vogesella* is not a common genus found in drinking water treatment plants or commonly referred to in other studies on BAC. However, as *Vogesella* has been isolated from natural water and soil (Jørgensen et al., 2010; Sheu et al., 2013; Subhash et al., 2013; Rameshkumar et al., 2016), they may appear in the drinking water treatment facilities. Compared to the research results of Lu et al. (2020), the dominant genus differs significantly in this study that used the same types of GAC under the same operating parameters, with the only difference being feed water. The differences in microbial characteristics were likely due to differences in quality of feed water, which in this study was the solution of humic acid from the Shanxi weathered-coal seam.

3.5.3 Vertical community structure

The characteristics of the vertical community structure were observed through samples from different heights of the 1# and 3# BAC columns (Figs. 5(c)–5(f)). The phylogenetic relationship between the middle and bottom samples was closer than their relationship with the surface layer, which resulted from a high load of water influent. Among the dominant genera, *Acinetobacter* and *Pseudomonas* tended to take up smaller proportions with increasing depth; they may be strains with relatively strong load resistance. In contrast, *Nitrospira*, which accounted for a higher proportion at the bottom than at the top, was speculated to have weak resistance to high organic load.

4 Conclusions

Although a high iodine value and micropore volume do not guarantee a high total removal efficiency during the stable stage of BAC operation, they do influence the removal efficiency of different organic fractions. The removal mechanism for carbon with high micropore volume and low micropore volume is also different; BAC with a high iodine value removes small MW organics more effectively.

The removal characteristics and mechanism are related to the pore structure of GAC. The micropore volume of GAC determines the removal capacity of BAC with regard to molecules with low MW, part of which are correspondingly microbial by-products. The removal of molecules with higher MW is related to the community structure of the biofilm, which is related to the pore structure. However, the effects of the pore structure on the biofilm community need to be further researched.

The volume of super-macropores (D>100 μm) is consistent with the biomass density and biodiversity. However, biomass density and biodiversity do not affect the removal characteristics.

Other microbiological results include: the community structure of the BAC biofilm varies with GAC type and depth of the sample in the column, and the biodiversity of samples is related more to the GAC type than its position in the column. The dominant genera are largely determined by the influent water quality.

It should be noted that the selection criteria for GAC may vary based on different water bodies, though the organic removal mechanisms for different water bodies are similar. However, it can be concluded from this study that for water with different characteristics, it is feasible to use pore structure as the criterion for the selection of the type of carbon for use in water purification systems.

Acknowledgements This study was supported by the National Key R&D Program of China (No. 2019YFC0408700), the funds from the National Natural Science Foundation of China (Grant Nos. 51778323 and 51761125013), and the National Science and Technology Major Projects of China (Nos. 2012ZX07404-002, 2017ZX07108-002, and 2017ZX-07502003).

Electronic Supplementary Material Supplementary material is available in the online version of this article at https://doi.org/10.1007/s11783-021-1419-1 and is accessible for authorized users.

References

Boon N, Pycke B F, Marzorati M, Hammes F (2011). Nutrient gradients in a granular activated carbon biofilter drives bacterial community organization and dynamics. Water Research, 45(19): 6355–6361

Chen M, Liu W, Tan G, Han L (2013). Study on the influential factors on expansion curves of up-flow GAC process in waterworks. Water and Wastewater Engineering, 39(3): 115–120 (in Chinese)

Chen S, Zhou Y, Chen Y, Gu J (2018). Fastp: An ultra-fast all-in-one FASTQ preprocessor. Bioinformatics (Oxford, England), 34(17): i884–i890

Chen W, Westerhoff P, Leenheer J, Booksh K (2003). Fluorescence excitation-emission matrix regional integration to quantify spectra for dissolved organic matter. Environmental Science & Technology, 37 (24): 5701–5710

Chiang Y C, Chiang P C, Huang C P (2001). Effects of pore structure and temperature on VOC adsorption on activated carbon. Carbon, 39 (4): 523–534

Du Z, Jia R, Li C, Cui P, Song W, Liu J (2020). Pilot-scale UV/H_2O_2-BAC process for drinking water treatment – Analysis and comparison of different activated carbon columns. Chemical Engineering Journal, 382: 123044

Dussert W B, Stone V R G (1994). Biological activated carbon process

for water purification. Water-Engineering & Management, 141(12): 22–24

Edgar R C (2013). UPARSE: highly accurate OTU sequences from microbial amplicon reads. Nature Methods, 10(10): 996–998

Franz M, Arafat H A, Pinto N G (2000). Effect of chemical surface heterogeneity on the adsorption mechanism of dissolved aromatics on activated carbon. Carbon, 38(13): 1807–1819

Gibert O, Lefevre B, Fernandez M, Bernat X, Paraira M, Pons M (2013). Fractionation and removal of dissolved organic carbon in a full-scale granular activated carbon filter used for drinking water production. Water Research, 47(8): 2821–2829

Han L, Liu W, Chen M, Zhang M, Liu S, Sun R, Fei X (2013). Comparison of NOM removal and microbial properties in up-flow/down-flow BAC filter. Water Research, 47(14): 4861–4868

Herzberg M, Dosoretz C G, Kuhn J, Klein S, Green M (2006). Visualization of active biomass distribution in a BGAC fluidized bed reactor using GFP tagged Pseudomonas putida F1. Water Research, 40(14): 2704–2712

Hidayah E N, Chou Y C, Yeh H H (2016). Using HPSEC to identify NOM fraction removal and the correlation with disinfection by-product precursors. Water Science and Technology: Water Supply, 16 (2): 305–313

Hou L, Zhou Q, Wu Q, Gu Q, Sun M, Zhang J (2018). Spatiotemporal changes in bacterial community and microbial activity in a full-scale drinking water treatment plant. Science of the Total Environment, 625: 449–459

Jiang W, Xia S, Liang J, Zhang Z, Hermanowicz S W (2013). Effect of quorum quenching on the reactor performance, biofouling and biomass characteristics in membrane bioreactors. Water Research, 47 (1): 187–196

Jørgensen N O G, Brandt K K, Nybroe O, Hansen M (2010). Vogesella mureinivorans sp. nov., a peptidoglycan-degrading bacterium from lake water. International Journal of Systematic and Evolutionary Microbiology, 60(10): 2467–2472

Kaarela O E, Harkki H A, Palmroth M R T, Tuhkanen T A (2015). Bacterial diversity and active biomass in full-scale granular activated carbon filters operated at low water temperatures. Environmental Technology, 36(6): 681–692

Karanfil T, Kilduff J (1999). Role of granular activated carbon surface chemistry on the adsorption of organic compounds. 1. Priority pollutants. Environmental Science & Technology, 33(18): 3217–3224

Klimenko N, Winther-Nielsen M, Smolin S, Nevynna L, Sydorenko J (2002). Role of the physico-chemical factors in the purification process of water from surface-active matter by biosorption. Water Research, 36(20): 5132–5140

Korotta-Gamage S M, Sathasivan A (2017). A review: Potential and challenges of biologically activated carbon to remove natural organic matter in drinking water purification process. Chemosphere, 167: 120–138

Lautenschlager K, Hwang C, Ling F, Liu W T, Boon N, Koster O, Egli T, Hammes F (2014). Abundance and composition of indigenous bacterial communities in a multi-step biofiltration-based drinking water treatment plant. Water Research, 62: 40–52

Liao X, Chen C, Wang Z, Wan R, Chang C H, Zhang X, Xie S (2013a). Changes of biomass and bacterial communities in biological activated carbon filters for drinking water treatment. Process Biochemistry, 48(2): 312–316

Liao X, Chen C, Wang Z, Wan R, Chang C H, Zhang X, Xie S (2013b). Pyrosequencing analysis of bacterial communities in drinking water biofilters receiving influents of different types. Process Biochemistry, 48(4): 703–707

Lillo-Ródenas M A, Cazorla-Amorós D, Linares-Solano A (2005). Behaviour of activated carbons with different pore size distributions and surface oxygen groups for benzene and toluene adsorption at low concentrations. Carbon, 43(8): 1758–1767

Liu C, Yang J, Li C, Zhou K, Liu Y, Gao Z, Chen W (2019). The variation of the biological activated carbon during the application and the judgement criterion of its invalidation. Water & Wastewater Engineering, 45(2): 9–16 (in Chinese)

Liu S T, Yang H W, Liu W J, Zhao Y, Wang X M, Xie Y F F (2016). Evaluation of backwash strategies on biologically active carbon filters by using chloroacetic acids as indicator chemicals. Process Biochemistry, 51(7): 886–894

Lu Z, Sun W, Li C, Ao X, Yang C, Li S (2019). Bioremoval of non-steroidal anti-inflammatory drugs by *Pseudoxanthomonas* sp. DIN-3 isolated from biological activated carbon process. Water Research, 161: 459–472

Lu Z, Sun W, Li C, Cao W, Jing Z, Li S, Ao X, Chen C, Liu S (2020). Effect of granular activated carbon pore-size distribution on biological activated carbon filter performance. Water Research, 177: 115768

Magoč T, Salzberg S L (2011). FLASH: fast length adjustment of short reads to improve genome assemblies. Bioinformatics (Oxford, England), 27(21): 2957–2963

McKie M J, Bertoia C, Taylor-Edmonds L, Andrews S A, Andrews R C (2019). Pilot-scale comparison of cyclically and continuously operated drinking water biofilters: Evaluation of biomass, biological activity and treated water quality. Water Research, 149: 488–495

Moore B C, Cannon F S, Westrick J A, Metz D H, Shrive C A, DeMarco J, Hartman D J (2001). Changes in GAC pore structure during full-scale water treatment at Cincinnati a comparison between virgin and thermally reactivated GAC. Carbon, 39(6): 789–807

Morlay C, Joly J P (2010). Contribution to the textural characterisation of Filtrasorb 400 and other commercial activated carbons commonly used for water treatment. Journal of Porous Materials, 17(5): 535–543

Newcombe G, Drikas M, Hayes R (1997). Influence of characterised natural organic material on activated carbon adsorption effect on pore volume distribution and adsorption of 2-methylisoborneol. Water Research, 31(5): 1065–1073

Oh S, Hammes F, Liu W T (2018). Metagenomic characterization of biofilter microbial communities in a full-scale drinking water treatment plant. Water Research, 128: 278–285

Pharand L, Van Dyke M I, Anderson W B, Huck P M (2014). Assessment of biomass in drinking water biofilters by adenosine triphosphate. Journal- American Water Works Association, 106(10): E433–E444

Qi W, Li W, Zhang J, Wu X, Zhang J, Zhang W (2018). Effect of biological activated carbon filter depth and backwashing process on transformation of biofilm community. Frontiers of Environmental Science & Engineering, 13(1): 1–11

Rameshkumar N, Lang E, Tanaka N (2016). Description of *Vogesella oryzae* sp. nov., isolated from the rhizosphere of saline tolerant pokkali rice. Systematic and Applied Microbiology, 39(1): 20–24

Ross P S, van der Aa L T J, van Dijk T, Rietveld L C (2019). Effects of water quality changes on performance of biological activated carbon (BAC) filtration. Separation and Purification Technology, 212: 676–683

Servais P, Billen G, Bouillot P (1994). Biological colonization of granular activated carbon filters in drinking- water treatment. Journal of Environmental Engineering, 120(4): 888–899

Sheu S Y, Chen J C, Young C C, Chen W M (2013). Vogesella fluminis sp. nov., isolated from a freshwater river, and emended description of the genus *Vogesella*. International Journal of Systematic and Evolutionary Microbiology, 63(Pt_8): 3043–3049

Stackebrandt E, Goebel B M (1994). Taxonomic note: A place for DNA-DNA reassociation and 16S rRNA sequence analysis in the present species definition in bacteriology. International Journal of Systematic Bacteriology, 44(4): 846–849

Subhash Y, Tushar L, Sasikala C, Ramana C V (2013).Vogesella alkaliphila sp. nov., isolated from an alkaline soil, and emended description of the genus *Vogesella*. International Journal of Systematic and Evolutionary Microbiology, 63(Pt_6): 2338–2343

Wang Q, Garrity G M, Tiedje J M, Cole J R (2007). Naive Bayesian classifier for rapid assignment of rRNA sequences into the new bacterial taxonomy. Applied and Environmental Microbiology, 73 (16): 5261–5267

Wu Z, Zhang P, Zeng G, Zhang M, Jiang J (2012). Humic acid removal from water with polyaluminum coagulants: Effect of sulfate on aluminum polymerization. Journal of Environmental Engineering, 138(3): 293–298

Xu B, Gao N Y, Sun X F, Xia S J, Simonnot M O, Causserand C, Rui M, Wu H H (2007). Characteristics of organic material in Huangpu River and treatability with the O_3-BAC process. Separation and Purification Technology, 57(2): 348–355

Yang J, Ma J, Song D, Zhai X, Kong X (2016). Impact of preozonation on the bioactivity and biodiversity of subsequent biofilters under low temperature conditions; A pilot study. Frontiers of Environmental Science & Engineering, 10(4): 5–10

Yang S D, Liao L H, Liu Z D (2014). Effect of temperature and the altitude of filler on biological activated carbon performance. Applied Mechanics and Materials, 621: 13–18

Yapsaklı K, Çeçen F, Aktaş Ö, Can Z S (2009). Impact of surface properties of granular activated carbon and preozonation on adsorption and desorption of natural organic matter. Environmental Engineering Science, 26(3): 489–500

Yu Y (2015). Impacts of Activated Carbon Porosity Feature on the Removal and Microbiological Characteristics of BAC. Dissertation for the Master's Degree. Beijing: Tsinghua University (in Chinese)

Zheng J, Lin T, Chen W, Tao H, Tan Y, Ma B (2018). Removal of precursors of typical nitrogenous disinfection byproducts in ozonation integrated with biological activated carbon (O_3/BAC). Chemosphere, 209: 68–77